Asian Journal of Scientific Research

ISSN 1992-1454

science alert
http://www.scialert.net

ANSInet
an open access publisher
http://ansinet.com

Asian Journal of Scientific Research 6 (2): 146-156, 2013
ISSN 1992-1454 / DOI: 10.3923/ajsr.2013.146.156

Performance Evaluation of Solar Driven Activated Carbon Fiber-Ethanol based Adsorption Cooling System in Malaysia

[1]Khairul Habib and [2,3]Bidyut B. Saha

[1]Department of Mechanical Engineering, Universiti Teknologi PETRONAS, Bandar Seri Iskandar, 31750 Tronoh, Perak, Malaysia

[2]Department of Mechanical Engineering, Kyushu University, 744 Motooka, Nishi-ku, Fukuoka 819-0395, Japan

[3]International Institute for Carbon-Neutral Energy Research (WPI-I2CNER), Kyushu University, 744 Motooka, Nishi-ku, Fukuoka 819-0395, Japan

Corresponding Author: Khairul Habib, Department of Mechanical Engineering, Universiti Teknologi PETRONAS, Bandar Seri Iskandar, 31750 Tronoh, Perak, Malaysia

ABSTRACT

This study presented a theoretical analysis of the performance of a two-bed solar driven activated carbon fiber-ethanol adsorption chiller designed for Malaysian climate. This innovative adsorption chiller employs pitch based activated carbon fiber as adsorbent and ethanol as refrigerant. A simulation program has been developed for modeling and performance evaluation for the solar driven adsorption cooling cycle using the meteorological data of Kuala Lumpur, Malaysia. The optimum cooling capacity and Coefficient of Performance (COP) are calculated in terms of adsorption/desorption cycle time and regeneration temperature. Results indicate that the adsorption chiller is feasible even when low-temperature heat source is available. Results also show that the adsorption cycle can achieve a cooling capacity of 12 kW when the heat source temperature is about 85°C.

Key words: Solar energy, adsorption system, carbon fiber, ethanol, regeneration temperature

INTRODUCTION

Solar radiation is known to be the largest and the world's most abundant, permanent and clean energy source. Compared to the annual global energy use, the amount of solar radiation intercepted by the earth's surface is much higher. In recent years, many promising technologies have been developed to extract sun's energy (Mechlouch and Brahim, 2008; El Genidy, 2012; Al-Salihi *et al*., 2010). One of these important technologies is the solar cooling systems which employ either absorption or adsorption technologies. In the last few decades thermally powered adsorption cooling systems have attracted much attention as they appear to be promising from the view point of greenhouse gas emissions and ozone layer depletion problems. Chlorofluorocarbons (CFCs) and Hydro-chlorofluorocarbons (HCFCs) have been considered as the major contributors to the environmental hazard. Adsorption cooling cycles are considered as environmentally benign, having zero Ozone Depletion Potential (ODP) due to the use of natural refrigerants or alternative refrigerants of CFCs and HCFCs. The other advantages of adsorption cooling systems are that they are free of vibrations as they do not have any moving parts, simple control and lower operation cost.

The working pairs of adsorption cooling and heat pump are mainly dominated by silica gel-water (Chua *et al.*, 1999), zeolite-water (Wang *et al.*, 2006), activated carbon-ammonia (Miles and Shelton, 1996) and activated carbon-methanol (Anyanwu and Ezekwe, 2003) pairs.

In the adsorption cooling system, the use of water and methanol as refrigerant makes those possible to be powered by solar energy below 100°C. However, the water based adsorption cooling system requires the development of very low vacuum system and the uptake of water on porous adsorbent is limited usually up to 40% of dry adsorbent mass (Chua *et al.*, 2002). The reason for using activated carbon fiber has been mentioned elsewhere (Hamamoto *et al.*, 2006). The use of solar driven adsorption refrigeration system has been mentioned in the literature (Pons and Guilleminot, 1986).

From the above perspective, the present study deals with the analytical investigation of the performance of a two-bed Activated Carbon Fiber (ACF)-ethanol adsorption cooling cycle. This novel cycle is driven by solar energy and the analysis of solar thermal system is carried out with the TRNSYS software using the meteorological data of Kuala Lumpur. A cycle simulation computer program of the novel adsorption cooling system is developed to analyze the cooling capacity and COP variations by varying adsorption/desorption cycle times and regeneration temperatures.

MATERIALS AND METHODS

Working principle of ACF-ethanol adsorption cooling cycle: Figure 1 shows the schematic diagram of the two-bed adsorption cooling cycle. The cycle comprises of four heat exchangers namely, evaporator (eva.), condenser (cond.) and two sorption elements (SE 1 and SE 2). The description of the ACF-ethanol adsorption chiller has been presented by Saha *et al.* (2007).

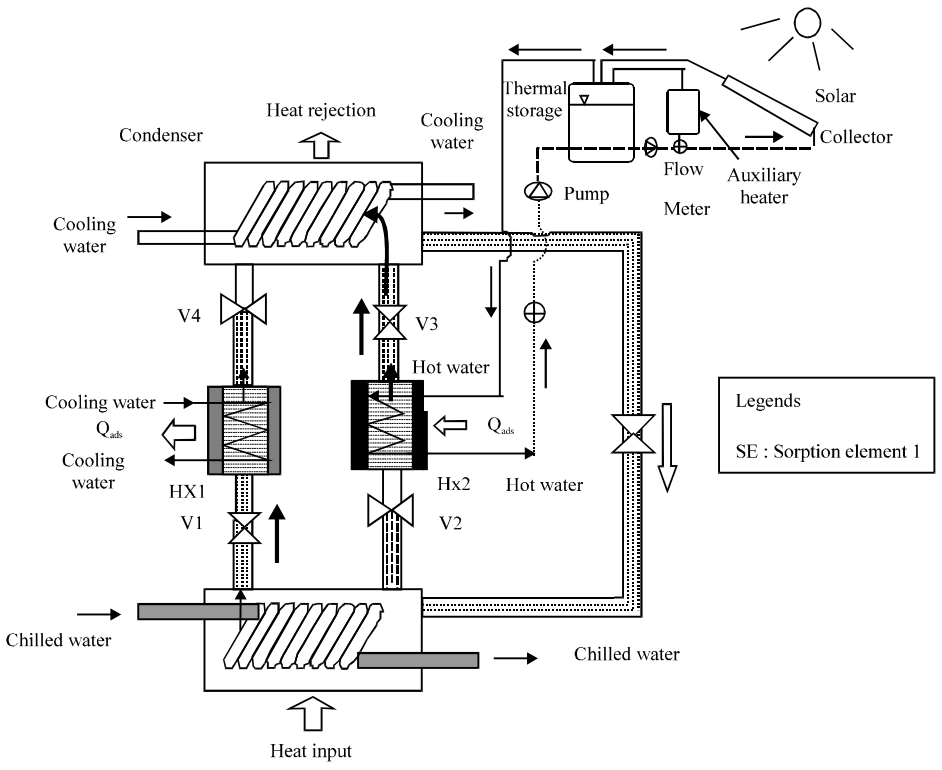

Fig. 1: Schematic diagram of solar driven ACF-ethanol adsorption cooling

Mathematical modeling

Adsorption isotherms: The Dubinin-Radushkevich (D-R) equation is used to estimate the equilibrium uptake of ACF-ethanol pair:

$$x = x_0 \exp\left\{-D\left[T \ln\left(\frac{P_s}{P}\right)\right]^2\right\} \tag{1}$$

The numerical values of x_0 and D of ACF-ethanol are evaluated experimentally and are found to be 0.797 kg ethanol kg^{-1} ACF, 1.716×10-6 K^{-2}, respectively (Saha *et al.*, 2007).

Adsorption kinetics: Adsorption rate is estimated by using the well known Linear Driving Force (LDF) equation (Saha *et al.*, 2007):

$$\frac{\partial x}{\partial t} = 15 D_{so} \frac{\exp\left(\frac{-E_a}{RT}\right)}{R_p^2}(x^* - x) \tag{2}$$

The numerical values of D_{so} and E_a for ACF-ethanol pair are found to be 1.8×10^{-12} m^2 sec^{-1} and 306.7×10^3 J kg^{-1}, respectively (Saha *et al.*, 2007).

Isosteric heat of adsorption: The isosteric heat of adsorption for ACF-ethanol pair can be expressed as (Saha *et al.*, 2007):

$$\Delta H_{st} = h_{fg} + E\left[\left\{\ln\left(\frac{x_0}{x^*}\right)\right\}^{\frac{1}{n}} + a\left(\frac{T}{T_c}\right)^b\right] \tag{3}$$

For ACF-ethanol system, the values of a and b are 6.72 and 9.75, respectively.

Solar collector energy balance: The energy balance of the energy balance of the evacuated tube collector can be expressed as (Duffie and Beckman, 1991):

$$mC_{pf}(T_{out}\text{-}T_{in}) = A_C F_R (I(\tau\alpha)\text{-}UL(T_{in}\text{-}T_{amb}) \tag{4}$$

Energy balance of combined cycle

Adsorption/desorption energy balance: Using the lumped approach the energy balance of sorption bed for ACF-ethanol cycle can be expressed as (Habib *et al.*, 2011):

$$\left[m_{acf}C_{p,acf} + m_{acf}C_p^{eth}x^{eth} + m_{Al}C_{p,Al} + m_{Cu}C_{p,Cu}\right]\frac{dT_{ads/des}^{eth}}{dt} = \delta m_{acf}\left\{h_g\left(P_{eva/cond}^{eth}, T_{ads/des}^{eth}\right) - h_g\left(T_{eva/cond}^{eth}\right) + \Delta H_{st}^{eth}\right\}\frac{dx_{ads/des}^{eth}}{dt} + \dot{m}_w C_{p,w}\left(T_{w,in,ads/des}^{eth} - T_{w,o,ads/des}^{eth}\right) \tag{5}$$

For a small temperature difference across heating/cooling fluid such as water, the outlet temperature of the source is sufficiently accurate to be modeled by the Log Mean Temperature Difference (LMTD) method and it is given by:

$$T_{w,o,bed}^{eth} = T_{bed}^{eth} + \left(T_{w,in,bed}^{eth} - T_{bed}^{eth}\right)\exp\left[-\frac{(UA)_{bed}^{eth}}{\left(\dot{m}C_p\right)_w}\right] \tag{6}$$

Evaporator energy balance: The evaporator energy balance of ACF-ethanol cycle can be expressed as (Habib *et al*., 2011):

$$\left[m_{eva}^{eth}C_{p,eva} + m_{hex}C_{p,Cu}\right]\frac{dT_{eva}^{eth}}{dt} = -\delta\left\{h_g\left(P_{eva}^{eth}, T_{ads}^{eth}\right) - h_g\left(T_{eva}^{eth}\right) + h_{fg}^{eth}\right\}m_{acf}\frac{dx_{ads}^{eth}}{dt} + \left(\dot{m}C_p\right)_{chill}\left(T_{chill,in} - T_{chill,o}\right) \tag{7}$$

The water outlet temperature can be expressed as:

$$T_{chill,o} = T_{eva}^{eth} + \left(T_{chill,in} - T_{eva}^{eth}\right)\exp\left[-\frac{(UA)_{eva}^{eth}}{\left(\dot{m}C_p\right)_w}\right] \tag{8}$$

Condenser energy balance: The condenser energy balance of ACF-ethanol cycle can be written as (Habib *et al*., 2011):

$$(m_{cond}^{eth}C_{p,cond} + m_{hex}^{eth}C_{p,Cu})\frac{dT_{cond}^{eth}}{dt} = -\delta\left\{h_g\left(P_{cond}^{eth}, T_{des}^{eth}\right) - h_g\left(T_{cond}^{eth}\right) + h_{fg}^{eth}\right\}m_{acf}\frac{dx_{des}^{eth}}{dt} + \dot{m}_w C_{p,w}\left(T_{w,in,cond}^{eth} - T_{w,o,cond}^{eth}\right) \tag{9}$$

The condenser outlet temperature can be expressed as:

$$T_{w,o,cond}^{eth} = T_{cond}^{eth} + \left(T_{w,in,cond}^{eth} - T_{cond}^{eth}\right)\exp\left[-\frac{(UA)_{cond}^{eth}}{\left(\dot{m}C_p\right)_w}\right] \tag{10}$$

Cooling capacity: The cooling capacity is obtained at the evaporator of ACF-ethanol cycle:

$$Q_{eva}^{cycle} = \frac{1}{t_{cycle}}\int_0^{t_{cycle}}\left(\dot{m}C_p\right)_w\left(T_{chill,in} - T_{chill,o}\right)dt \tag{11}$$

Coefficient of performance: The Coefficient of Performance (COP) of adsorption cycle can be expressed as:

$$COP = \frac{\int_0^{t_{cycle}}(\dot{m}c_p)_{chill}\left(T_{chill,in} - T_{chill,o}\right)dt}{\int_0^{t_{cycle}}(\dot{m}c_p)_{des}\left(T_{h,in} - T_{h,o}\right)dt} \tag{12}$$

Here, t_{cycle} denotes the total cycle time.

Weather data: An accurate climatic database is required in solar energy technologies. In this regard, the accuracy of solar radiation and ambient air temperature is important. The

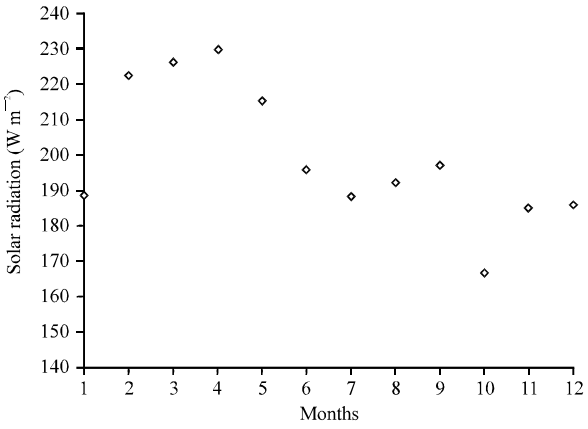

Fig. 2: Variation of solar radiation of Kuala Lumpur through out the year

climatic data based on the typical year concept for Kuala Lumpur, Malaysia (latitude = 3.167 and longitude = 101.7) has been used in the present study. Figure 2 shows the variation of solar radiation of Kuala Lumpur throughout the year according to the meteorological data of Kuala Lumpur. It is observable from Fig. 2 that the maximum solar radiation is achieved in the month of April (around 230 W m^{-2}) in Kuala Lumpur.

RESULTS AND DISCUSSION

Hot water supply: Figure 3 depicts the hot water supply from the tank to the combined cycle for Kuala Lumpur climate during 6 am to 6 pm, May. It can be seen from Fig. 3 that at 10 am the temperature of the hot water is around 60°C and the maximum temperature of the hot water is achieved from 12-2 pm and the temperature is around 85°C.

Chiller transient response: Figure 4 shows the chiller temporal histories for all the components (adsorber, desorber, evaporator and condenser) by using the mathematical model presented herein. Table 1 depicts the rated conditions for adsorption cycle. The values of the symbols used in the present simulation model are furnished in Table 2 (Saha *et al.*, 2007). Inlet temperatures of hot and cooling water are taken as 85 and 30°C, respectively. The chilled water inlet temperature is taken as 14°C. It can be seen from Fig. 4, the ACF-ethanol single-stage adsorption chiller is able to reach from transient to nearly steady state within three half cycles or 1890 sec, where adsorption/desorption cycle time is taken as 600 sec and switching time is taken as 30 sec.

Figure 5 shows the outlet temperature profiles for heat transfer fluids. The cooling water outlet temperature from the adsorber after 600 sec the adsorption/desorption cycle time is about 3°C higher than the coolant inlet temperature and the hot water outlet temperature from the desorber is about 2.7°C lower than the hot water inlet temperature.

Adsorption/desorption cycle time: The simulated results of cooling capacity and COP variations with adsorption/desorption cycle for the standard heat transfer fluid temperatures and flow rates conditions are shown in Fig. 6. The switching (pre-heating or pre-cooling) time is chosen as 30 sec.

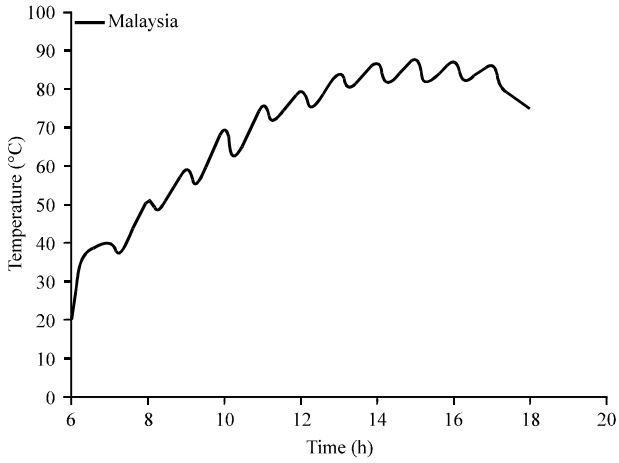

Fig. 3: Variation of temperature during hot water supply Kuala Lumpur in May, 2011

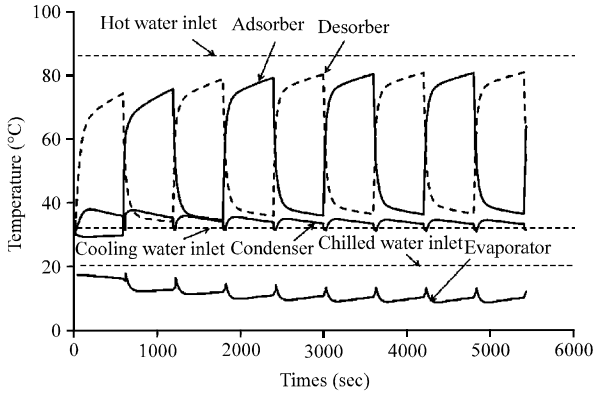

Fig. 4: Temperature profile of various components of ACF-ethanol cycle

Table 1: Rated conditions

Hot water inlet		Cooling water inlet		Chilled water inlet	
Temperature (°C)	Flow rate (kg sec^{-1})	Temperature (°C)	Flow rate (ads+cond) (kg sec^{-1})	Temperature (°C)	Flow rate (kg sec^{-1})
85	1.5	30	(1.5+1.5)	14	0.7

Half cycle time: 630 sec, Adsorption/desorption cycle time: 600 sec, Switching time: 30 sec

Table 2: Values adopted for simnlation

Symbols	Values
m_{acf}	60 kg
UA_{bed}	2952 W kg^{-1}
UA_{eva}	4870 W kg^{-1}
UA_{cond}	15330 W kg^{-1}
m_{cond}	24.28 kg
m_{eva}	12.45 kg
$C_{p,ac}$	930 J kg^{-1} K^{-1}
$C_{p,Al}$	904 J kg^{-1} K^{-1}
$C_{p,Cu}$	386 J kg^{-1} K^{-1}

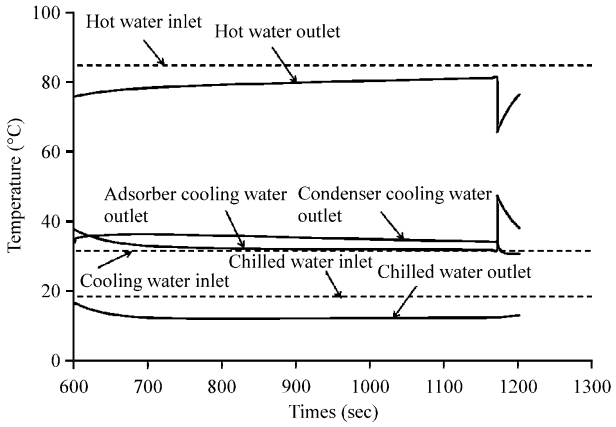

Fig. 5: Outlet temperature profile of heat transfer fluids of ACF-ethanol adsorption cooling cycle

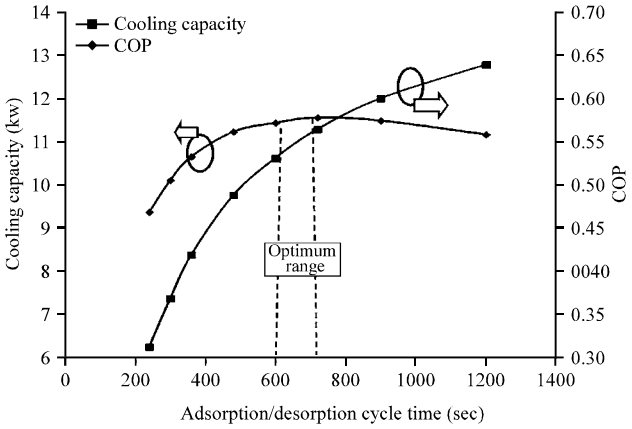

Fig. 6: Effects of adsorption/desorption cycle time on cooling capacity and COP

From Fig. 6, it is observed that the highest cooling capacity for the adsorption cycle achieved in the evaporator is around 11.55 kW for cycle times between 600 and 700 sec. As can be seen from Fig. 6, when the cycle time is shorter than 400 sec, it is not sufficient for adsorption or desorption satisfactorily. As a result, cooling capacity decreases abruptly. On the other hand, when cycle time is longer than 720 sec, the cooling capacity decreases gradually due to the less intense of adsorption after the first 10 min as the adsorbent reaches towards equilibrium. It can be seen from Fig. 6 that COP increases uniformly with longer adsorption/desorption cycle time. However, after around 900 sec, the increase in COP and chiller efficiency values becomes marginal. The optimum value of COP is around 0.55 when the adsorption/desorption cycle time is between 600 and 700 sec.

Operating temperatures: Figure 7 shows the effects of regeneration temperature on cooling capacity and COP with fixed cooling water and chilled water inlet temperatures. It can be seen from Fig. 7 that the cooling capacity increases linearly from 2.83 to 14.5 kW with heat source temperature varies from 60 to 85°C. This is due to the amount of refrigerant circulation increases

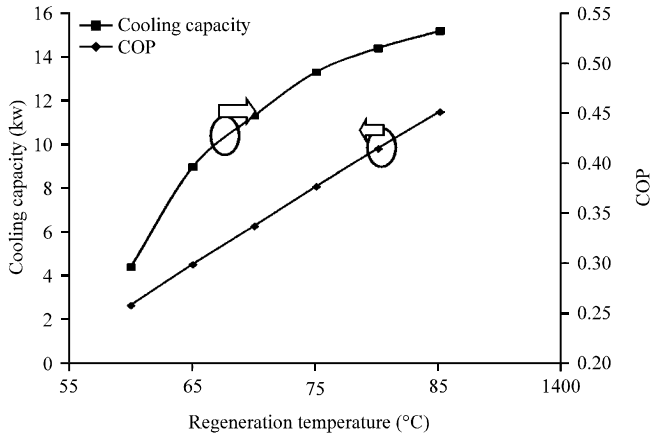

Fig. 7: Effects of regeneration temperature on cooling capacity and COP

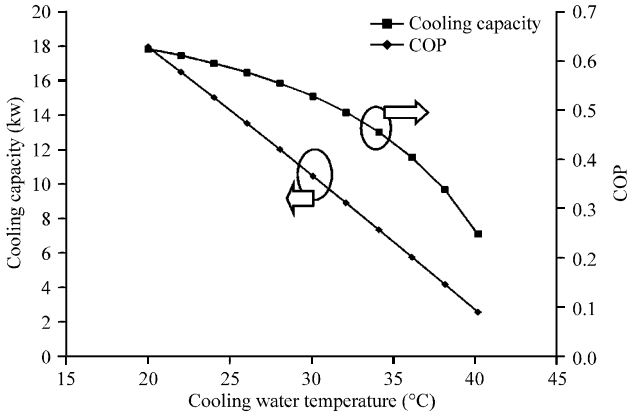

Fig. 8: Effects of cooling water inlet temperature on cooling capacity and COP

when the amount of desorbed refrigerant increases with the higher driving heat source temperature. With the increase of hot water temperature the simulated COP values also increase and reach a peak value between 80 to 85°C. The optimum COP value is 0.53 for hot water inlet temperature between 80 and 85°C in combination with the coolant inlet temperature at 30°C. The variation of cooling capacity and COP with inlet cooling water temperature of ACF-ethanol adsorption cooling cycle is shown in Fig. 8. It is observable from Fig. 8 that cooling capacity increases steadily from 2 to 18 kW with the decrease of cooling water inlet temperature from 40 to 20°C. This is due to the fact that lower adsorption temperatures result in larger amounts of refrigerant being adsorbed and desorbed during each cycle. The simulated COP values decrease with the increase of cooling water inlet temperature.

Figure 9 shows the effects of chilled water inlet temperature on cooling capacity and COP with fixed hot and cooling water inlet temperature. It is visible from Fig. 9 that both the cooling capacity and COP increase with the increase of chilled water inlet temperature.

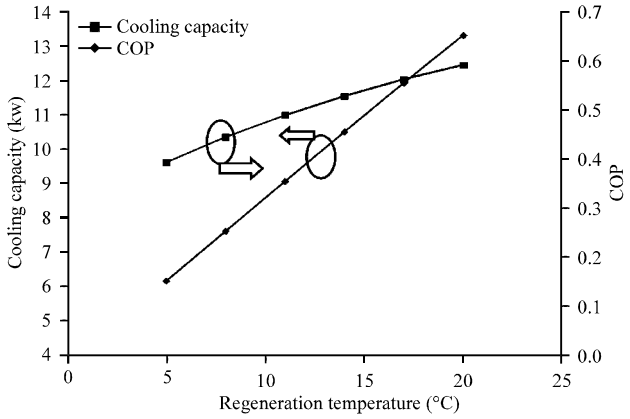

Fig. 9: Effects of chilled water inlet temperature on cooling capacity and COP

CONCLUSIONS

This study investigated analytically the performance of ACF-ethanol adsorption chiller driven by solar energy using a cycle simulation model. The solar system is modeled with TRNSYS program using the weather conditions of Kuala Lumpur. The prime advantage of ACF-ethanol adsorption cooling cycle is its ability to utilize low temperature heat (from 60 to 85°C) obtained from solar energy as the driving heat source with a coolant at 30°C. The simulation results show that the cooling capacity increases with the increase of regeneration temperature with a fixed cooling water temperature. Both cooling capacity and COP decrease with higher coolant inlet temperatures. Cooling capacity and COP also increase with higher chilled water inlet temperature. The present study can be useful to design activated carbon based adsorption cycles driven by solar energy suitable for Malaysia and other tropical climates.

NOMENCLATURE

A	=	Area (m^2)
A_c	=	Collector area (m^2)
COP	=	Coefficient of performance (-)
C_p	=	Specific heat capacity (J kg^{-1} K^{-1})
D_s	=	Surface diffusion coefficient (m^2 s^{-1})
D_{so}	=	Pre-exponential constant (m^2 s^{-1})
E_a	=	Activation energy (J kg^{-1})
H	=	Enthalpy (J kg^{-1})
m	=	Mass (kg)
$\dot{m}$	=	Mass flow rate (kg sec^{-1})
P	=	Pressure (Pa)
P_s	=	Saturation pressure (Pa)
Q	=	Power (W)
Q_u	=	Useful energy gain from collector (W)
R	=	Gas constant (J kg^{-1} K^{-1})
R_p	=	Adsorbent fiber radius (m)
T	=	Temperature (°C or K)

t	=	Time (sec)
U	=	Overall heat transfer coefficient (W m^{-2} K^{-1})
U_L	=	Overall heat transfer coefficient of collector to ambient (W m^{-2} K^{-1})
F_R	=	Collector heat removal factor
I	=	Incident solar radiation (W m^{-2})
$\tau\alpha$	=	Effective transmittance-absorptance product (-)
W	=	Volumetric uptake (m^3 kg^{-1})
W_0	=	Limiting volumetric uptake (m^3 kg^{-1})
E	=	Characteristic energy (J kg^{-1})
n	=	Heterogeneity constant (-)
x	=	Instantaneous uptake (kg kg^{-1})
x*	=	Equilibrium uptake (kg kg^{-1})
x_0	=	Limiting adsorption uptake (kg kg^{-1})
ΔH_{st}	=	Isosteric heat of adsorption (J kg^{-1})
η	=	Efficiency (-)

Subscripts:

ac	=	Activated carbon
amb	=	Ambient
ads	=	Adsorber
bed	=	Sorption heat exchanger (adsorber/desorber)
chill	=	Chilled water
cond	=	Condenser
col	=	Collector
des	=	Desorber
eva	=	Evaporator
f	=	Liquid phase
g	=	Gaseous phase
h	=	Hot water
in	=	Inlet
o	=	Outlet
w	=	Water

Superscripts:

eth	=	Ethanol

REFERENCES

Al-Salihi, A.M., M.M. Kadum and A.J. Mohammed, 2010. Estimation of global solar radiation on horizontal surfaces using routine meteorological measurements for different cities in Iraq. Asian J. Sci. Res., 3: 240-248.

Anyanwu, E.E. and C.I. Ezekwe, 2003. Design, construction and test run of a solid adsorption solar refrigerator using activated carbon/methanol as adsorbent/adsorbate pair. Energy Conv. Manage., 44: 2879-2892.

Chua, H.T., K.C. Ng, A. Chakraborty, N.M. Oo and M.A. Othman, 2002. Adsorption characteristics of silica gel + water system. J. Chem. Eng. Data, 47: 1177-1181.

Chua, H.T., K.C. Ng, A. Malek, T. Kashiwagi, A. Akisawa and B.B. Saha, 1999. Modeling the performance of two-bed, silica gel-water adsorption chiller. Int. J. Refrig., 22: 194-204.

Duffie, J.A. and W.A. Beckman, 1991. Solar Engineering of Thermal Processes. 2nd Edn., Wiley, New York.

El Genidy, M.M., 2012. Multiple linear regression formula for the probability of the average daily solar energy using the queue system. Asian J. Mathe. Statistics, 5: 93-98.

Habib, K., B.B. Saha, A. Chakraborty, S. Koyama and K. Srinivasan, 2011. Performance evaluation of combined adsorption refrigeration cycle. Int. J. Refrig., 34: 129-137.

Hamamoto, Y., K.C.A. Alam, B.B. Saha, S. Koyama, A. Akisawa and T. Kashiwagi, 2006. Study on adsorption refrigeration cycle utilizing activated carbon fibers. Part 1. Adsorption characteristics. Int. J. Refrig., 29: 305-314.

Mechlouch, R.F. and A.B. Brahim, 2008. A global solar radiation model for the design of solar energy systems. Asian J. Sci. Res., 1: 231-238.

Miles, D.J. and S.V. Shelton, 1996. Design and testing of a solid sorption heat-pump system. Applied Therm. Eng., 16: 389-394.

Pons, M. and J.J. Guilleminot, 1986. Design of an experimental solar powered, solid adsorption ice maker. J. Solar Energy Eng., 103: 2514-2523.

Saha, B.B., I.I. El-Sharkawy, A. Chakraborty and S. Koyama, 2007. Study on an activated carbon fiber-ethanol adsorption chiller: Part I-system description and modeling. Int. J. Refrig., 30: 86-95.

Wang, D.C., Z.Z. Xia and J.Y. Wu, 2006. Design and performance prediction of a novel zeolite-water adsorption air conditioner. Energy Conv. Manage., 47: 590-610.